

promoting access to White Rose research papers



Universities of Leeds, Sheffield and York
<http://eprints.whiterose.ac.uk/>

This is the published version of an article in the **Journal of Geophysical Research D: Atmospheres, 115 (11)**

White Rose Research Online URL for this paper:

<http://eprints.whiterose.ac.uk/id/eprint/76612>

Published article:

Emmel, C, Knippertz, P and Schulz, O (2010) *Climatology of convective density currents in the southern foothills of the Atlas Mountains*. Journal of Geophysical Research D: Atmospheres, 115 (11). D11115. ISSN 0148-0227

<http://dx.doi.org/10.1029/2009JD012863>



Climatology of convective density currents in the southern foothills of the Atlas Mountains

C. Emmel,^{1,2} P. Knippertz,^{1,3} and O. Schulz⁴

Received 21 July 2009; revised 6 November 2009; accepted 25 January 2010; published 15 June 2010.

[1] Density currents fed by evaporationally cooled air are an important dust storm-generating feature and can constitute a source of moisture in arid regions. Recently, the existence of such systems has been demonstrated for the area between the High Atlas Mountains and the Sahara desert in southern Morocco on the basis of case studies. Here, a climatological analysis is presented that uses data from the dense climate station network of the IMPETUS project (An Integrated Approach to the Efficient Management of Scarce Water Resources in West Africa) for the 5 year period 2002–2006. Objective criteria mainly based upon abrupt changes in wind and dew point temperature are defined to identify possible density current situations. The preselected events are then subjectively evaluated with the help of satellite imagery and surface observations to exclude causes for air mass changes other than moist convective cold pool formation. On average, 11 ± 4 density currents per year are detected with the main season lasting from April to September. Density currents occur mainly in the afternoon and evening due to the diurnal cycle of moist convection. Mean changes at the leading edge are increases in 2 m dew point temperature and wind speed by 5.4°C and 8.2 m s^{-1} , respectively, and a decrease in 2 m air temperature of 2.3°C . The High Atlas and Jebel Saghro are found to be the most important source regions, while only a few systems originate over the Saharan lowlands. Labilization of the atmosphere due to upper-level troughs over northwest Africa and an enhanced moisture content favor density current formation. In addition, detailed case studies representative of different density current types are presented.

Citation: Emmel, C., P. Knippertz, and O. Schulz (2010), Climatology of convective density currents in the southern foothills of the Atlas Mountains, *J. Geophys. Res.*, 115, D11115, doi:10.1029/2009JD012863.

1. Introduction

[2] Desert dust contributes substantially to the Earth's aerosol budget [Textor *et al.*, 2006]. The Sahara desert is the largest source of mineral dust and is responsible for almost half of the dust deposition to the world's oceans [Middleton and Goudie, 2001]. Saharan dust can be transported far beyond Africa and has been detected in remote regions such as northern Europe [Franzén *et al.*, 1994], Amazonia [Swap *et al.*, 1992], and the Caribbean Sea [Garrison *et al.*, 2003]. The region of Western Sahara–southern Morocco has an important impact on dust transport to western Europe

[Goudie and Middleton, 2001]. Mineral dust plays an important role in climatic and ecological processes, for example through its effects on radiation [Forster *et al.*, 2007], cloud microphysics [e.g., Min *et al.*, 2009], nutrient supply to the oceans [Jickells *et al.*, 1998] and continents [Goudie and Middleton, 2001] as well as through transporting disease-spreading spores [Shinn *et al.*, 2000].

[3] Several meteorological phenomena have been associated with dust emission reaching from small-scale dust devils and convective plumes [Koch and Renno, 2005; Ansmann *et al.*, 2009] over mesoscale convective cold pools [Idso *et al.*, 1972; Knippertz *et al.*, 2007; Marsham *et al.*, 2008; Flamant *et al.*, 2007] to synoptic-scale systems such as lee cyclones [Knippertz *et al.*, 2009a]. The cold pools are formed through evaporation of precipitation in sufficiently dry subcloud layers and then spread horizontally due mainly to the hydrostatic forces arising from gravity and the density differences to the ambient air, which are usually on the order of a few percent only [Simpson, 1997]. The strong and gusty winds at the leading edge of these so called ‘density currents’ can lift up dust to heights of more than 1500 m forming dramatic ‘dust walls’ that have been called ‘haboobs’ in

¹Institute for Atmospheric Physics, Johannes Gutenberg University of Mainz, Mainz, Germany.

²Now at Department of Earth and Ocean Sciences, University of British Columbia, Vancouver, British Columbia, Canada.

³Now at Institute for Climate and Atmospheric Science, Faculty of Environment, School of Earth and Environment, University of Leeds, Leeds, UK.

⁴Geographical Institute, University of Bonn, Bonn, Germany.

various desert regions [Sutton, 1925; Freeman, 1952; Lawson, 1971; Idso et al., 1972; Membery, 1985; Offer and Goossens, 2001; Chen and Fryrear, 2002; Knippertz et al., 2007; Flamant et al., 2007; Miller et al., 2008; Williams et al., 2008]. Density currents are generally characterized by the existence of a near-surface feeder flow implying that the wind velocity behind the leading edge is higher than the propagation velocity of the current [Smith and Reeder, 1988]. The arrival of the leading edge is usually characterized by a sudden decrease in temperature and visibility, an increase in dew point temperature and wind speed, and often by a change in the direction of the wind [Knippertz et al., 2007; Miller et al., 2008]. The strong turbulent winds and low visibility at the leading edge can pose a threat to aviation and destroy infrastructure on the ground [Sutton, 1925; Miller et al., 2008]. After the passage, the wind direction usually becomes steadier [Sutton, 1925]. At least in some desert areas, density currents are more frequent during summer months in close connection with the annual cycle of moist convection [Sutton, 1925; Miller et al., 2008].

[4] Knippertz et al. [2007] first described the occurrence of dust-lifting, extended density currents in the southern foothills of the Moroccan High Atlas based on the 5 week period of the Saharan Mineral Dust Experiment (SAMUM) [Heintzenberg, 2009] in May–June 2006. They suggest that the Atlas Mountain range serves as a trigger for initiating deep moist convection [see also Hübener and Kerschgens, 2007], especially in situations of high moisture content and low vertical stability, often in connection with a nearby upper-level trough. If there is northwesterly shear, hydrometeors sediment into the lower layers at the dry side of the mountains where evaporation can be quite substantial, leading to the formation of a large cold pool. It has been shown in idealized numerical experiments that the strongest low-level ascent occurs on the downshear side of a cold pool [e.g., Weisman and Rotunno, 2004, Figure 6]. Knippertz et al. [2009b] find that in situations with westerly shear this uplift can regenerate moist convection on the Saharan side of the Atlas causing the cold pool to propagate eastward with a squall-line-type convective organization.

[5] Due to the occurrence of density currents in remote and data-sparse areas like the Sahara, most studies on their characteristics are based upon few cases and/or few point measurements. Therefore the multiyear observations from the fairly dense network of several automatic weather stations in southern Morocco run by the IMPETUS project (An Integrated Approach to the Efficient Management of Scarce Water Resources in West Africa) represents a particularly valuable data source for the study of density currents. The major goals of this study are (1) to identify density currents from this unique data set, (2) to compile a detailed climatology including aspects such as interannual variability, diurnal and annual cycle, location of origin and track, typical values of the change in atmospheric conditions at the leading edge, and propagation velocity, and (3) to determine the synoptic preconditions for their development. Section 2 contains information on the data, while the methodology is discussed in section 3. The climatological results will be presented in section 5 after a discussion of two detailed case studies on representative density currents, which serve to

better illustrate the climatological findings (section 4). A summary and conclusions are given in section 6.

2. Data

[6] The main data employed for the analysis are observations from the network operated by the German research initiative IMPETUS in southern Morocco. This network consists of eleven automatic weather stations that are distributed between the highest peaks of the High Atlas (maximum height above 4000 m) across the parallel mountain chain of the Anti Atlas including Jebel Saghro and Jebel Ougnat with the highest altitudes of approximately 2500 m down to the border with Algeria, mainly following the course of the rivers Dadès and Drâa. The focus here is mainly on the stations southward of 31°N, namely Bou Skour (BSK), Arguioun (ARG), El Miyit (EMY), Jebel Brâhim (JHB), and Iriki (IRK; see Figure 1d), where most of the annual precipitation usually falls during just a few events. Measured parameters are, among others, air temperatures (T_a) and dew point temperatures (T_d) at 2 m, wind speed (wv) and direction (wd) at 3 m, as well as precipitation (p). When only relative humidity (rh) was given, T_d was calculated according to Lawrence [2005]. The data have a temporal resolution of 10 min or 15 min and are available for the years 2002–2006 with a few occasional gaps. Further information on the measuring equipment and locations is given by Knippertz et al. [2007], Schulz and de Jong [2004] and Schulz and Judex [2008].

[7] In addition, twice-daily atmospheric soundings from the nearest available WMO station at Bechar (31.62°N, 2.23°W, western Algeria) are taken from the archive of the University of Wyoming (<http://weather.uwyo.edu/upperair/sounding.html>) to assess vertical wind profiles and stability. This station is at a distance of about 450 km from the main study region and can therefore only give a rough idea of the conditions there. Three hourly surface observations from the SYNOP stations Errachidia (31.93°N, 4.40°W) and Ouarzazate (30.93°N, 6.90°W) are also considered for the synoptic analysis. For the investigation of cloud development, standard infrared (IR, 10.8 μm channel) satellite imagery from METEOSAT is employed. To characterize the synoptic-scale environment, fields of 300 hPa geopotential height (Z300), mean sea level pressure (MSLP), and total column water (q_{col}) from the operational analyses of the European Centre for Medium-Range Weather Forecasts (ECMWF) in $1^\circ \times 1^\circ$ resolution at 1200 UTC are considered. All anomalies are calculated with respect to monthly means over the study period 2002–2006.

3. Methodology

3.1. Objective Identification Criteria

[8] Thresholds for specified variables are set to preselect possible density current situations out of the IMPETUS data set, mainly following the case study results by Knippertz et al. [2007]: (1) the dew point temperature (T_d) has to increase by at least 4°C in 30 min; (2) the mean wind speed (wv_{mean}) during the T_d jump and the following hour needs to be at least 4 m s⁻¹; and (3) no rain is allowed to fall between 1 h before and 1 h after the T_d jump. A temperature criterion was initially considered, too, but proved to be of

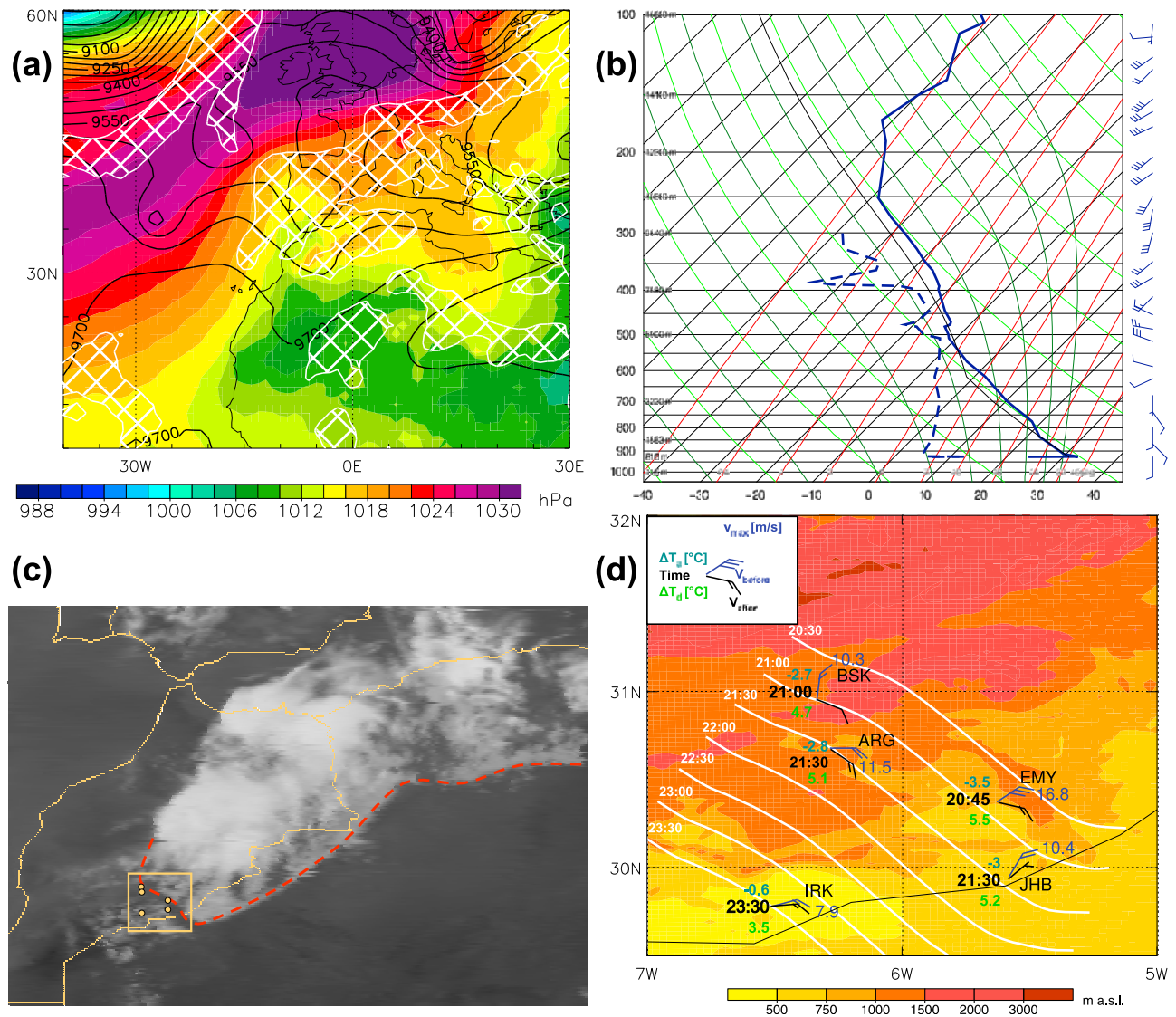


Figure 1. Synoptic situation on 14 July 2006. (a) MSLP (shading), Z300 (black contours every 50 gpm), and the anomaly of $q_{\text{col}} \geq 4$ mm (white cross-hatching) at 1200 UTC. (b) Skew-T/log-P diagram for 1200 UTC at Bechar (dashed line marks T_d , and solid line marks T_a). (c) IR satellite image at 2100 UTC with the leading edge marked in red. The box indicates the study region, and the dots indicate the southern IMPETUS stations. (d) Frontal analysis in white every 30 min with station observations depicted according to the legend in the top left corner: black is time of passage, turquoise and green are half-hourly changes in T_a and T_d , respectively, blue and black barbs are 1.5 h mean wind speed ending with and starting with the passage time, respectively, with the pertinent prevalent wind direction (WMO convention), and blue is maximum wind speed during the 1.5 h after approach of the leading edge. Station names are abbreviated as in section 2, and the topography is shaded.

little use, as the temperature at 2 m is too strongly affected by sensible heat fluxes from the ground and nocturnal surface inversions [see Knippertz *et al.*, 2007]. The rain criterion was introduced to exclude cases, in which precipitation at a given station causes a T_d jump and gusty, variable winds, but where a coherent leading edge propagation was often hard to determine. Of course, the rains might generate such a feature outside of our study region, but this cannot be examined with the available data. Most density currents in the study by Knippertz *et al.* [2007] occurred without being followed by rain at the considered IMPETUS stations, suggesting that this criterion has a lim-

ited impact. Tests with higher or lower T_d thresholds (e.g., 5°C in 15 min) resulted either in the preselection of too many cases for the subsequent subjective evaluation or in density currents not being registered that were clearly identifiable from satellite imagery, respectively. An additional spatial criterion (4) is introduced to only preselect cases of a certain horizontal extent over the study region: The criteria 1–3 formulated above have to be met at least at two stations within the following time intervals, which mainly reflect the distances between the stations: ARG–BSK, EMY–JHB 3 h; JHB–IRK 4 h; EMY–IRK 5 h; ARG–EMY, BSK–EMY 6 h; ARG–JHB, BSK–JHB 7 h; ARG–IRK, BSK–IRK 10 h.

These time windows are large enough to allow the consideration of very slow systems (on the order of 3.5 m s^{-1}). This procedure resulted in a preselection of 141 possible events. In addition, 35 events fulfilling criteria 1–3 at EMY only were selected to account for 1 year data gap at JHB between June 2005 and June 2006.

3.2. Subjective Evaluation

[9] Unfortunately the objective criteria discussed above proved to be insufficient to unambiguously distinguish evaporationally driven density currents from air mass changes brought about by other phenomena. Therefore an additional subjective evaluation is carried out on the basis of IR satellite imagery and station maps displaying observations from the IMPETUS stations. The satellite images are examined in high temporal resolution in order to verify the emergence of an assumed density current from an area of deep moist convection. The temperature difference between the cold pool and its surroundings is reflected in different IR signal during daytime. During the night the IR contrast often vanishes due to the strong radiational cooling of the surface in the surroundings, which are usually characterized by lower dust content and weaker winds. An additional hint to track a possible cold pool are arc clouds that often form above the leading edge, where warmer ambient air is lifted above the density current head [Knippertz *et al.*, 2007]. The station maps are used to evaluate the spatiotemporal coherency in the changes in T_d , T_a , and wind speed over the study region. This latter analysis was at times problematic due to influences of the orography (ARG for example is located in a rather narrow valley) and surface inhomogeneities (desert-oasis circulation). This procedure eliminated almost 70% of the preselected cases, for which the moisture increase could mostly be traced back to a transport of marine air masses from the Mediterranean Sea or the Atlantic Ocean instead. The final set of 54 clearly identifiable density currents is then classified into currents originating from the Atlas Mountains and those having their emergence over the Sahara to the east or south of the study region.

[10] In addition, the station chart analyses are used to subjectively determine the propagation velocity for selected events with well-defined leading edges. Previous studies have used the following theoretical relation to calculate the propagation velocity: $U = (gH\Delta\rho/\rho)^{0.5}$ with ρ being the density of the surrounding air, $\Delta\rho$ the density difference between the air masses, g the acceleration of gravity, and H the height of the current [Simpson, 1997]. In such studies, H is estimated by assuming a hydrostatic pressure change due to the arrival of the cold air as reflected in the surface temperature measurements. This approach is not possible in our case since pressure measurements with a sufficient resolution are not available.

4. Case Studies

[11] In this section two case studies of density currents representative of the two main regions of origin will be presented. The first case in July 2006 is an intense and extended example of the rather common case of moist convection being triggered over the Atlas Mountains, while the second case in September 2003 has its origin in the Sahara, a starting point that is less frequent.

4.1. An Atlas Mountain Case

[12] At 1200 UTC 14 July 2006 an upper-level trough reaches from the Iberian Peninsula into the northwestern Sahara (black lines in Figure 1a). The MSLP field indicates a slight northward extension of the Saharan heat low toward the Atlas Mountains (shading in Figure 1a). The 4 mm contour of the q_{col} anomaly shows relatively moist conditions along the southern side of the Atlas chain from southern Morocco to the Algerian-Tunisian border as well as to the southeast and east of the trough over the Sahara (white cross hatching in Figure 1a). The atmospheric sounding at Bechar for the same time indicates moist mid-levels and weakly stable layers around 800 and 480 hPa (Figure 1b). Further heating of the ground in the course of the afternoon can be expected and is the most likely trigger for the deep convective clouds reported by the station observer at 1500 UTC, albeit other factors might have contributed as well. The wind profile at Bechar shows light southerly and southeasterly winds up to 700 hPa and increasing, mainly westerly winds above this level. This vertical distribution is most likely associated with the Atlas pumping effect that results in a circulation from the forelands toward the mountains on high-radiation days [Flamant *et al.*, 2007]. The convergence of this flow over the mountain crests is an important mechanism for the initiation of moist convection. As explained in section 1, the westerly shear visible in Figure 1b will favor cold pool formation on the Saharan side of the Atlas.

[13] Around midday, IR satellite imagery shows first indications of convection over the High Atlas Mountains and a little later also over the Tell Atlas in northern Algeria, associated with the generation of several density currents during the following hours (not shown). Two smaller systems emerge around 1400 UTC from the Tell Atlas, while an extensive density current propagates away from the High Atlas to the northwest around 1800 UTC. Two of the high-mountain IMPETUS stations and the synoptic station at Errachidia in southeastern Morocco recorded light precipitation during the late afternoon and evening. By 2100 UTC the cold pools from the different convective cells have merged to form an about 1700 km long leading edge from central Morocco to the Algerian-Tunisian border (red line in Figure 1c). At this time, Bechar reports sustained winds of 15 m s^{-1} and dust mobilization near the station.

[14] The cold pool reaches the IMPETUS station EMY at 2045 UTC indicated by an increase in T_d by 5.5°C from 3.8°C to 9.3°C while T_a decreases by 3.5°C from 34.4°C to 30.9°C (Figure 1d). The mean wind speed ($w_{v,\text{mean}}$) doubles with the passage of the front to 15.2 m s^{-1} with the wind direction changing to ENE. The maximum wind speed ($w_{v,\text{max}}$) of 16.8 m s^{-1} (15 min mean) corresponds to 60 km h^{-1} and typically gusts on the order of 90 km h^{-1} can be expected. Within the following 45 min the leading edge reaches first BSK and then ARG and JHB, which all show similar but somewhat weaker changes than EMY. At IRK, where the front arrives at 2330 UTC, the observed change in T_d of 3.5°C is already lower than the criterion defined in section 3, but an abrupt jump is still visible. The small decrease in T_a of only 0.6°C might be related to the beginning nocturnal surface inversion [see Knippertz *et al.*, 2007; Flamant *et al.*, 2007]. The weaker wind signal and the fact that the leading

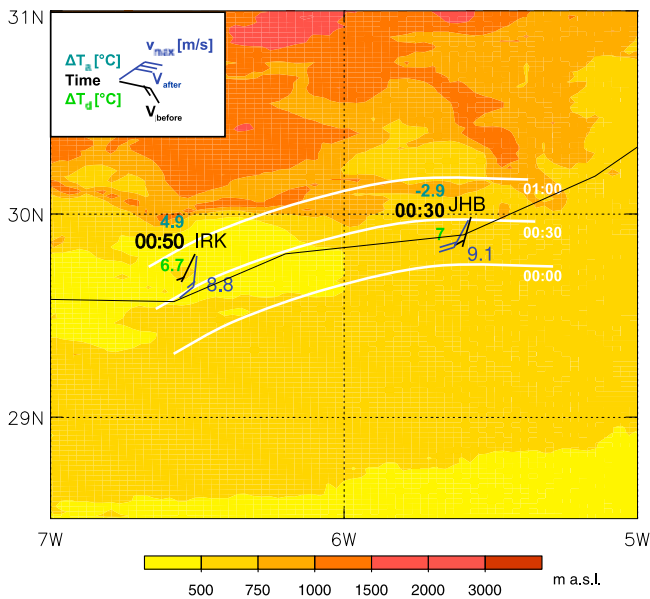


Figure 2. Same as Figure 1d but for 8 September 2003.

edge is hardly visible in satellite imagery suggest that the density current has reached its decay stage. The white lines in Figure 1d indicate the positions of the front between 2030 UTC and 2330 UTC as hand-analyzed on the basis of the observed wind direction, the time of passage, and the satellite imagery. The propagation velocity slows down from 11 m s^{-1} to 8.5 m s^{-1} near IRK. These values are considerably lower than the maximum wind speed at all stations excluding IRK in agreement with density current theory [Simpson, 1997] and observations in the Sahel [Lawson, 1971].

4.2. A Sahara Case

[15] In the early morning hours of 8 September 2003, the objective density current criteria set out in section 3 were fulfilled at the IMPETUS stations JHB and IRK, while the other stations were either not operating (ARG) or did not show any signs of a density current passage (BSK and EMY). Between 0030 UTC and 0100 UTC T_d at JHB increases from -1.5°C to 5.5°C , while T_a decreases from 34.0°C to 31.1°C (Figure 2). The wv_{mean} increases from 1.3 m s^{-1} to 7.7 m s^{-1} and the maximum wind speed behind the front reaches 9.1 m s^{-1} . IRK records similar signals in T_d , wv_{mean} , and wv_{max} about 20 min later. T_a rises from 28.0°C to 32.9°C with the arrival of the front indicating downward mixing of warmer air into the nocturnal inversion layer. This effect is most likely much more pronounced at IRK located in a dry lake bed than at the more elevated JHB where the temperature before the passage is much higher. Winds during the entire period are from the SSW suggesting front lines similar to what is depicted in white in Figure 2.

[16] Satellite imagery of 7 September shows a distinct deep convective cell with cold cloud tops moving from the border triangle of Algeria-Mauritania-Mali at 1700 UTC across northern Mauritania to the border with Western Sahara by 0100 UTC 8 September (Figure 3). A density current emanates from this convection in the late afternoon, traverses western Algeria, and brings about the air mass

changes recorded by the IMPETUS stations in southern Morocco (red lines in Figure 3). The initiation of the convection around 1400 UTC suggests that daytime heating has played an important role as a triggering mechanism in this relatively flat area (not shown). Figure 4 shows the synoptic situation at 1200 UTC 7 September and 24 h earlier. No distinct upper-level features were analyzed over the Sahara during this period in contrast to the cases discussed above and by Knippertz *et al.* [2007]. The MSLP field shows a low-pressure system that moves along 16°N from about 5°W to 10°W . Similar charts for the previous days indicate that this feature can be traced back to at least 5°E

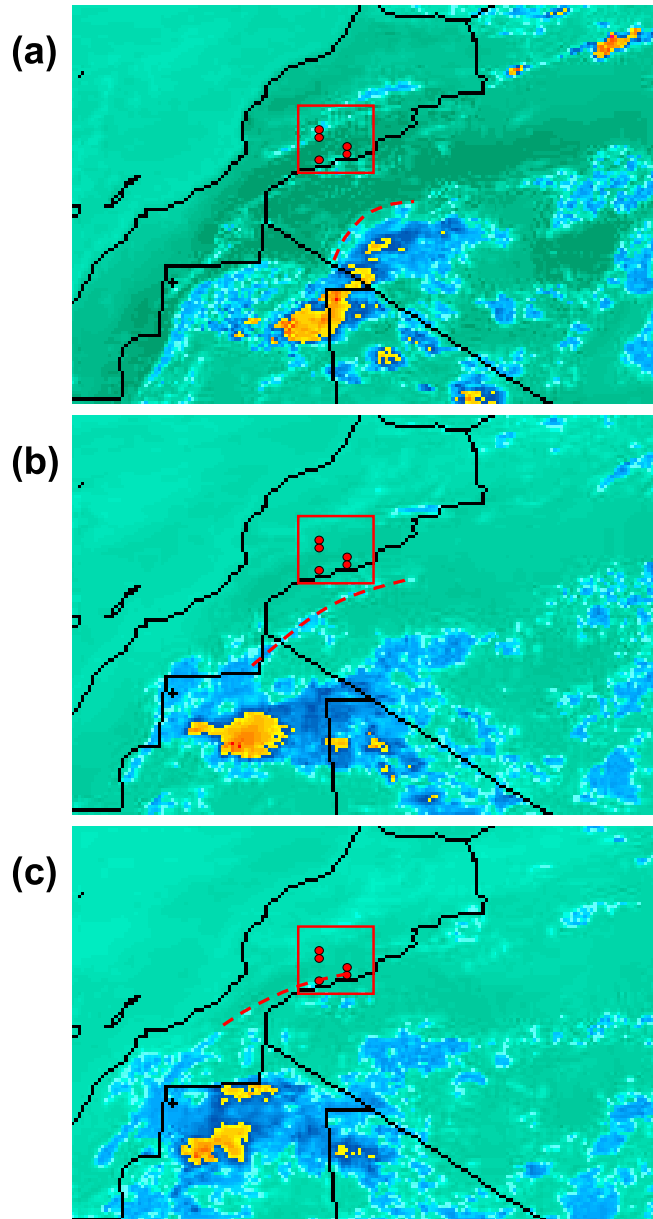


Figure 3. Same as Figure 1c but for 7 September 2003 at (a) 1700 UTC, (b) 2100 UTC, and (c) 8 September 2003 at 0100 UTC. The color scale for the infrared images reaches from dark green (cloud-free hot desert surface) over blue and yellow to red (cold cloud top).

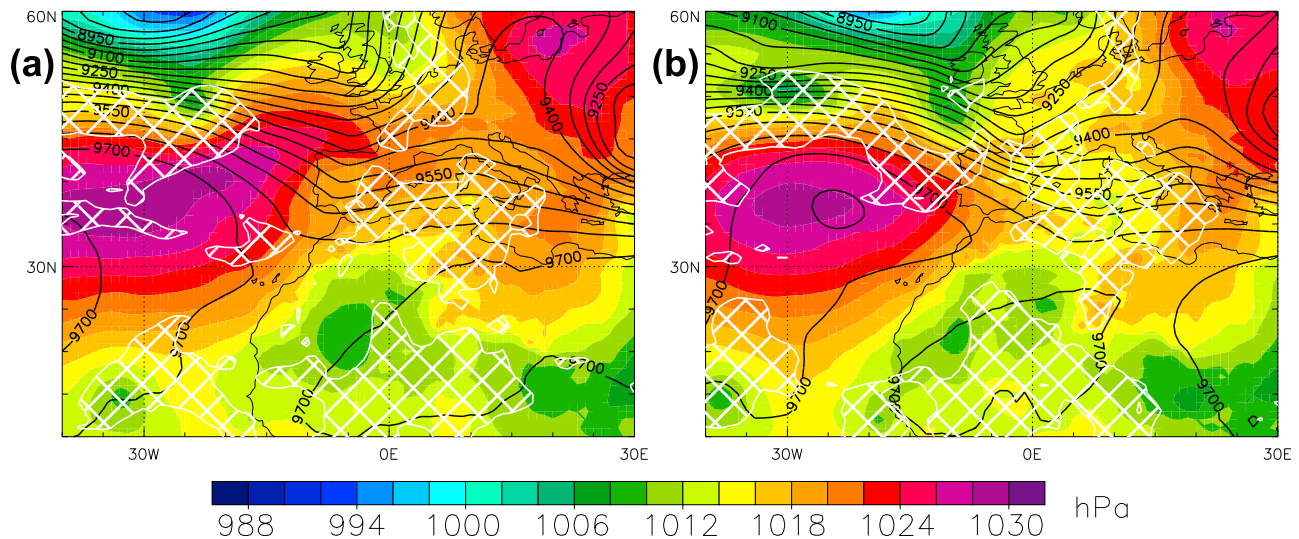


Figure 4. Same as Figure 1a but for 1200 UTC on (a) 6 and (b) 7 September 2003.

suggesting a possible connection to the trough of an African easterly wave. On the eastern side of the low, where the flow is southerly, q_{col} anomalies exceed 4 mm over an extended area (white cross hatching in Figure 4). This moist zone reaches the border triangle of Algeria-Mauritania-Mali around midday 7 September and provides the humidity necessary for the development of deep convection. This density current event characterized by moisture transport from the Sahel toward southern Morocco over

several days is similar to Case III from Knippertz *et al.* [2009a].

5. Climatology

5.1. Interannual, Seasonal, Diurnal, and Geographical Variations

[17] Figure 5a shows how the 54 identified density currents are distributed over the years from 2002 to 2006.

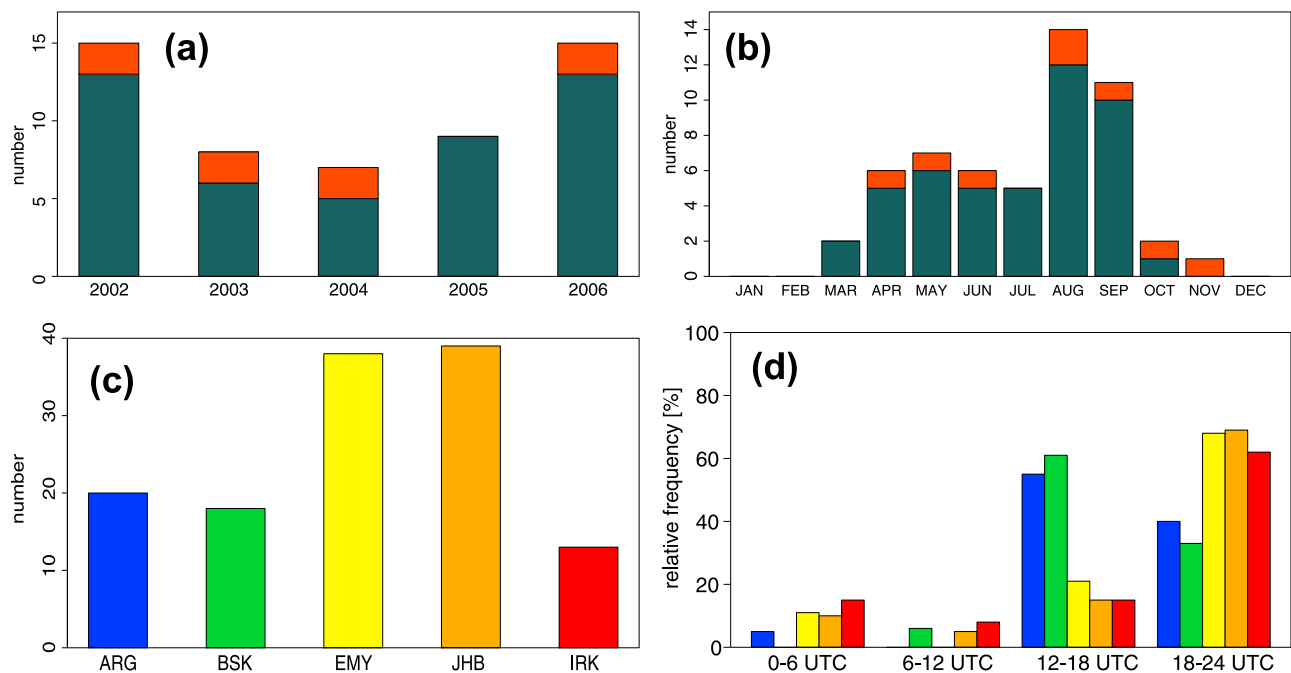


Figure 5. Density current climatology. (a) Year-to-year variability and (b) monthly distribution with dark gray (red) bars indicating density currents originating from the Atlas Mountains (the Sahara). (c) Total number and (d) normalized diurnal frequency at the five IMPETUS stations: ARG, blue; BSK, green; EMY, yellow; JHB, orange; and IRK, red.

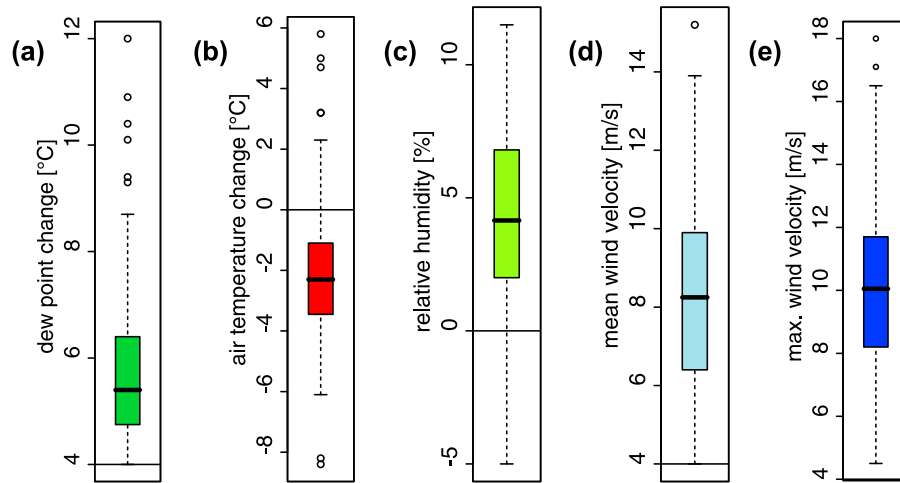


Figure 6. Box-and-whisker plots of the changes of (a) dew point temperature, (b) air temperature, and (c) relative humidity at the leading edge as well as the (d) mean and (e) maximum wind velocity behind the leading edge. Displayed are the median, the first quartile, the third quartile, and the smallest and largest nonoutlier values. Outliers are marked with open circles.

The interannual variability is relatively high with a mean of 11 density currents, a maximum of 15 in 2002 and 2006, and a minimum of seven in 2004. The most active month was August 2002 with five identified systems. The SAMUM field campaign in May–June 2006 was also a very active period [Knippertz *et al.*, 2007]. All years except 2005 had two density currents originating from the Sahara, resulting in a total of eight Sahara cases, while the majority of systems have their origin in the Atlas Mountains as expected from work by Knippertz *et al.* [2007] and the fact that the Atlas Mountains serve as a trigger for convection. The occurrence of density currents as defined here is clearly a phenomenon of the warm season with most systems occurring during April–October and no systems during December–February (Figure 5b). Between April and July, five to seven density currents per month were identified, while August and September show substantially higher numbers of 14 and 11, respectively. Potential reasons for this distinct annual cycle are closely related to the conditions necessary for triggering moist convection over the Atlas. Knippertz [2003] and Knippertz *et al.* [2003] showed that in late summer–early autumn, weak troughs in the upper westerlies frequently initiate a midlevel transport from the Sahel, which is moist at this time of the year, to the Atlas Mountains. In addition, the still high insolation leads to a robust Atlas pumping and ascent over the mountains, which provides a stable trigger for deep convection, if sufficient moisture is available. The Atlas pumping creates low-level flow toward the crest and a return flow aloft, leading to northwesterly shear on the Saharan side of the mountains. This shear is in some situations enhanced by the presence of upper-level troughs and favors propagation into the Saharan foreland as explained in section 1. Last but not least, the boundary layer is often deep and dry during summer, which allows substantial evaporation and an unimpeded subsidence of cooled air parcels to the ground.

[18] Figure 5c shows for how many of the 54 identified density currents the objective criteria set out in section 3.1 were fulfilled at each IMPETUS station. A large portion of the systems passed over the easternmost stations EMY

(37 events) and JHB (38 events), while ARG and BSK are only affected by 19 and 18 events, respectively. The southwesternmost station IRK shows the smallest number of occurrence of only 12. Potential reasons for this pattern are that (1) many density currents originate to the northeast of the region and affect EMY and JHB only (see also the discussion of Figure 7 below) and that (2) ARG and BSK are located in areas of complex topography, which might sometimes distort the leading edge passage through blocking and channeling. Being more elevated and further north, these stations are also more often affected by precipitation.

[19] The diurnal cycle of density current passage shows a clear maximum in the second half of the day at all stations (Figure 5d), most likely caused by the dependence of the parent moist convection on daytime heating. With the High Atlas being the most prominent source for density currents, the time of relative frequency maximum is shifted toward later hours with distance from the mountains. The northernmost stations ARG and BSK have their peak activity in the afternoon, while the other three stations show most activity in the evening. The lowest station IRK is, relatively speaking, more often affected after midnight than the other stations, although activity is low during this time of day.

5.2. Characteristics of the Leading Edge

[20] Figure 6 shows a statistical overview of the changes in various meteorological parameters at and behind the leading edge of the identified density currents in the form of box-and-whisker plots, which display the median, the first quartile, the third quartile, and the smallest and largest nonoutlier value. This statistical depiction was preferred to the computation of a mean and standard deviation as most of the variables do not show a Gaussian distribution. The median of the half-hourly change in T_d is 5.4°C (Figure 6a) and is not substantially higher than the lower bound of 4°C set by the objective selection criterion (see section 3.1). In 25% of all cases ΔT_d is larger than 6.3°C, while occasionally values as high as 12°C are recorded. The half-hourly change in T_a has a median of -2.3°C and an interquartile

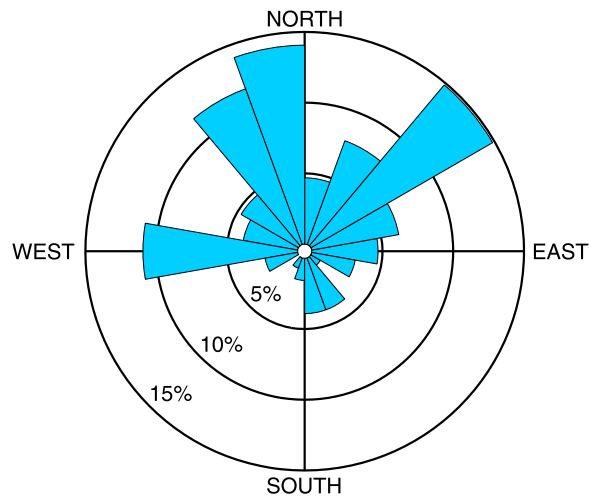


Figure 7. Wind rose of prevalent wind direction after the passage of the leading edge.

range of -3.5°C to -1.3°C (Figure 6b). Maximum cooling is -8.4°C . Interestingly, a considerable portion of leading edge passages are associated with a warming of up to 6°C , clearly indicating the effect of the downward mixing of warmer air into the nocturnal surface inversion mentioned earlier. Most of these cases (seven) were observed at IRK around midnight. The temperature changes presented here are on the same order as documented by Miller *et al.* [2008] for the Arabian Peninsula, while Lawson [1971] reports temperature drops of up to 15°C for the Sudan. The changes in T_d and T_a result in rh changes with a median of 4.15% and an interquartile range from 2.03% to 6.75% (Figure 6c). Maximum values of Δrh are -5% and 11.5% .

[21] The mean wind velocity wv_{mean} after the passage of the leading edge reach from 4 m s^{-1} (by design; see section 3.1) to 15.2 m s^{-1} with a median of 8.2 m s^{-1} and an interquartile range of $6.4\text{--}9.9\text{ m s}^{-1}$ (Figure 6d). The pertinent median and quartiles of wv_{max} are typically about 2 m s^{-1} larger than those of wv_{mean} with the highest observed value reaching 18 m s^{-1} (Figure 6e). A typical threshold for the lifting of dust from the ground is about 8 m s^{-1} [Chomette *et al.*, 1999]. Thus in 75% of the cases the 15 min mean wind speed is strong enough for dust mobilization, while in the remainder at least some gusts might exceed the threshold. The wind velocities are again similar to those reported by Miller *et al.* [2008] and Flamant *et al.* [2007]. The prevalent wind direction after passage of the leading edge is predominantly from westerly to northeasterly directions (Figure 7). In 15% of the cases the wind direction is northeasterly coming from the Jebel Saghro. For 26% of the density currents the wind blows from north-northwesterly directions from the northwestern parts of the Anti Atlas. The wind direction is westerly in 11% of the cases. The few cases showing wind directions from southwest to east with a small peak from SSE are probably a reflection of the eight density currents originating from the Sahara (Figure 5a). Although the wind is not always blowing exactly perpendicular to the leading edge due to, for example, effects of orography, the predominance of northerlies and northeasterlies points to the High Atlas and Jebel Saghro being the major source area for density currents.

5.3. Large-Scale Setting

[22] For the analysis of the synoptic situation accompanying the density current formation, a composite analysis was conducted. Anomalies of Z300, MSLP, and q_{col} with respect to monthly means were calculated for 1200 UTC on each density current day (DAY0) as well as for the analysis times 48 h earlier (DAY-2) and 24 h later (DAY+1). Then, means over all 54 systems were computed. On DAY-2, a weak negative MSLP anomaly of -1 hPa and a corresponding Z300 anomaly of -20 geopotential meters (gpm) are located to the west of Morocco, while a distinct anomalous troposphere-deep ridge is found over the northeastern Atlantic (Figure 8a). The q_{col} shows a weak positive anomaly to the east of the southern disturbance along the African Atlantic coast, indicating moisture transports from tropical Africa to the study area. Until DAY0 the MSLP/Z300 dipole moves slowly eastward accompanied by a slight intensification of the ridge (Figure 8b). The location of the negative Z300 anomaly right above Morocco and Algeria on DAY0 suggests that the convection generating the density current is favored by the labilization associated with cooler air at upper levels rather than by frontal lifting at the eastern side. A moist anomaly of up to 3 mm is almost colocated with the disturbance, which also supports moist convection. The MSLP is close to normal conditions suggesting a negligible role in the initiation process. The weak MSLP anomaly over tropical West Africa on DAY-2 and the enhanced q_{col} over the Sahara on DAY0 might be a reflection of the few Saharan cases (see discussion in section 4.2). On DAY+1 the negative Z300 anomaly has continued to move eastward to the Algerian Atlas (Figure 8c). Positive MSLP and q_{col} anomalies to the south of the High Atlas Mountains are most likely direct consequences of the density currents on the previous days. It is a sign of the quality of the ECMWF analyses to realistically represent these effects in such a data sparse region. It should be noted that the Z300 and MSLP anomalies over northwestern Africa are generally rather small, indicating that there is no dependence on one clearly defined synoptic setting. A subjective inspection revealed that only 70% of all DAY0s are characterized by a discernable upper-level trough, while in all other cases, most of which occur in August and September, daytime heating and high moisture contents appear to be enough to trigger convection (see the event discussed in section 4.2).

[23] To further characterize the conditions on density current days, the atmospheric soundings from Bechar are analyzed. In 70% of the cases the wind was blowing from southerly, southeasterly, or easterly directions in the layer between the ground and 700 hPa and predominantly from westerly directions at upper levels. This suggests that Atlas pumping was active on these days supporting the triggering of convection over the Atlas Mountains and the propagation to the Saharan side.

[24] The total number of density currents per year has been compared to the April–September mean index of the North Atlantic Oscillation (NAO). The linear correlation coefficient is -0.74 consistent with the projection of the MSLP composites on the negative phase of the NAO evident from Figure 8. Surprisingly the correlation for single months from April to September is not significant. A larger

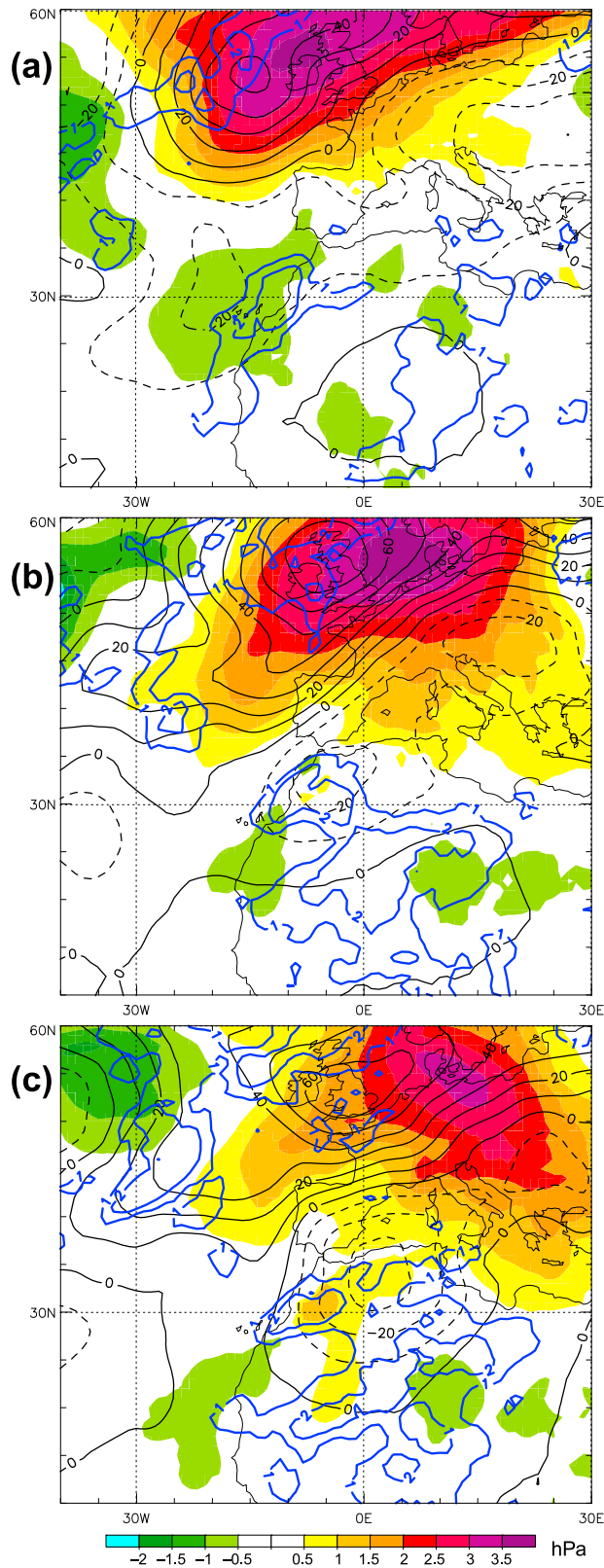


Figure 8. Composites of anomalies in MSLP (shaded), Z300 (black contours every 10 gpm), and q_{col} (blue, 1 and 2 mm contours only) on (a) DAY-2, (b) DAY0, and (c) DAY+1.

sample would be necessary to give a more significant statistics and to explore this relation further.

6. Summary and Conclusions

[25] Density currents caused by the evaporation of convective precipitation occur in many arid regions of the world. Despite their importance for dust mobilization and moisture transports they have not received much attention, not least because of a limited availability of good observations. This study contains the first detailed and statistically robust climatological analysis of density currents in the southern foothills of the Moroccan High Atlas. The unique data from a mesoscale network of eleven automatic weather stations located between the peaks of the High Atlas and the margin of the Sahara for the years 2002–2006 are the basis of this climatology and two detailed case studies. A relatively high temporal resolution of 15 min allows a reliable detection of potential events based upon the following objective criteria: (1) an increase in dew point temperature of at least 4°C in 30 min, (2) a sustained wind velocity of at least 4 m s^{-1} after the passage of the leading edge, (3) no rain during 2.5 h around the passage, and (4) fulfillment of criteria 1–3 at a minimum of two stations within a certain time window. This ensures that the identified systems are fairly intense, have a certain horizontal extension, and have traveled some distance from the precipitation source. As it turned out to be difficult to unambiguously distinguish convective density currents from the relatively frequent events of moist air transport from the Atlantic or the Mediterranean Sea with this method, the preselected cases were subsequently evaluated subjectively on the basis of satellite imagery and maps with the detailed station observations.

[26] With this analysis, 54 density currents were detected corresponding to a mean of eleven systems per year and a range of 7–15. Density currents are a phenomenon of the warm season with peak activity in August and September, when moist air from the Sahel is frequently transported to the Atlas region at midlevels [Knippertz, 2003; Knippertz *et al.*, 2003]. Most of the density currents occur in the afternoon or evening in close connection to the diurnal cycle of deep convection. The occurrence is shifted toward later hours with greater distance of the observing station to the High Atlas. The frequency decreases from northeast to southwest across the study region pointing to the High Atlas and the Jebel Saghro as the most important regions for initiation. Only about 8% of the identified systems originate from flatter terrain in the Sahara associated with moisture transport from the Sahel over several days, for example, in connection with the trough of an African easterly wave. Density currents propagating from the Atlas toward the desert transport air masses with elevated moisture content and therefore contribute to an input of humidity into the desert.

[27] The passage of the leading edge is associated with abrupt changes in meteorological conditions. Typical values are an increase in dew point temperature of 5.4°C (maximum 12°C), a decrease in temperature of -2.3°C , and mean wind speeds behind the leading edge of 8.2 m s^{-1} with 15 min maxima as high as 18 m s^{-1} , mostly from westerly, NNW, or northeasterly directions. Most systems generated winds strong enough to exceed typical thresholds for dust

mobilization. The large range in temperature changes at the leading edge from -8.4°C to $+5.0^{\circ}\text{C}$ is a reflection of the strong diurnal cycle in near-surface temperature due to the intense sensible heat fluxes during the day and strong radiation inversions at night, which are usually broken by the turbulent winds associated with the density currents. It was only possible to reliably determine the propagation velocity of a few density currents with the limited stations available. The estimated values cover a broad range of $3\text{--}11.1\text{ m s}^{-1}$. These characteristics compare well with studies in other arid regions [e.g., Lawson, 1971; Miller et al., 2008; Flamant et al., 2007].

[28] An analysis of the synoptic situation showed that the majority of the density currents are connected to an upper-level trough as suggested by Knippertz et al. [2007], while no clear connection to the surface pressure situation could be found. The upper disturbance is part of a north-south dipole that slowly moves eastward across northwest Africa and Europe around the day of the density current formation. There are indications that the trough favors midlevel moisture transports from tropical Africa into the Atlas region prior to that day and then supports the formation of deep convection through a labilization of the upper troposphere. Radiosonde observations at the Algerian station Bechar show easterly or southerly winds at low levels and westerlies at upper levels on most density current days. This indicates that elevated heat sources over the mountains generate convergence, ascent, and eventually deep convection, while the inflow of dry and neutrally stratified desert air favors evaporation and cold pool formation, as soon as convective towers get sheared to the Saharan side of the mountains. Some of these general findings, including the identification criteria, can most likely be applied to other regions with some modifications accounting for local factors such as orography and moisture sources. This way the present study has added to the knowledge of density currents in arid regions. A possible extension of this work in the future is to better quantify the role density currents play for the dust and moisture budgets on the basis of conventional and satellite observations as well as experiments with numerical models.

[29] **Acknowledgments.** This work was supported through the DFG Emmy Noether grant to P.K. (grant KN 581/2–3). The IMPETUS project is funded by the Federal German Ministry of Education and Research under grant 01 LW06001B and by the Ministry of Innovation, Science, Research and Technology of the federal state of Northrhine-Westfalia under grant 313-21200200. We would like to thank Andreas H. Fink (University of Cologne) for providing the SYNOP data and satellite images for the case study analysis, the German Weather Service for providing access to ECMWF data, and Heini Wernli and his group for their technical and scientific support. We also wish to thank the three anonymous reviewers for their positive evaluation of this work and their helpful comments that contributed to improving this paper.

References

- Ansmann, A., M. Tesche, P. Knippertz, E. Bierwirth, D. Althausen, D. Müller, and O. Schulz (2009), Vertical profiling of convective dust plumes in southern Morocco during SAMUM, *Tellus, Ser. B*, *61*, 340–353.
- Chen, W., and D. Fryrear (2002), Sedimentary characteristics of a haboob dust storm, *Atmos. Res.*, *61*(1), 75–85.
- Chomette, O., M. Legrand, and B. Marticorena (1999), Determination of the wind speed threshold for the emission of desert dust using satellite remote sensing in the thermal infrared, *J. Geophys. Res.*, *104*(D24), 31,207–31,215.
- Flamant, C., J.-P. Chaboureaud, D. Parker, C. Taylor, J.-P. Cammas, O. Bock, F. Timouk, and J. Pelon (2007), Airborne observations of the impact of a convective system on the planetary boundary layer thermodynamics and aerosol distribution in the inter-tropical discontinuity region of the West African Monsoon, *Q. J. R. Meteorol. Soc.*, *133*, 1175–1189.
- Forster, P., et al. (2007), Changes in atmospheric constituents and in radiative forcing, in *Climate Change 2007: The Physical Science Basis. Contribution of Working Group I to the Fourth Assessment Report of the Intergovernmental Panel on Climate Change*, edited by S. Solomon et al., pp. 129–234, Cambridge Univ. Press, Cambridge, U. K.
- Franzén, L., M. Hjelmroos, P. Källberg, E. Brorström-Lunden, S. Junnto, and A. Savolainen (1994), The yellow snow episode of northern Fennoscandia, March 1991—A case study of long-distance transport of soil, pollen and stable organic compounds, *Atmos. Environ.*, *28*(22), 3587–3604.
- Freeman, M. (1952), *Duststorms of the Anglo-Egyptian Sudan*, *Meteorol. Rep.* *11*, 22 pp., Her Majesty's Stn. Off., London.
- Garrison, V., E. Shinn, W. Foreman, D. Griffin, C. Holmes, C. Kellogg, M. Majewski, L. Richardson, K. Ritchie, and G. Smith (2003), African and Asian dust: From desert soils to coral reefs, *BioScience*, *53*(5), 469–480.
- Goudie, A., and N. Middleton (2001), Saharan dust storms: Nature and the consequences, *Earth Sci. Rev.*, *56*, 179–204.
- Heintzenberg, J. (2009), The SAMUM-1 experiment over Southern Morocco: Overview and introduction, *Tellus, Ser. B*, *61*, 2–11.
- Hübener, H., and M. Kerschgens (2007), Downscaling of current and future rainfall climatologies for southern Morocco. Part I: Downscaling method and current climatology, *Int. J. Climatol.*, *27*(8), 1065–1073.
- Idso, S., R. Ingram, and J. Pritchard (1972), An American haboob, *Bull. Am. Meteorol. Soc.*, *53*, 930–933.
- Jickells, T., S. Doring, W. Deuser, T. Church, R. Arimoto, and J. Prospero (1998), Air-borne dust fluxes to a deep water sediment trap in the Sargasso Sea, *Global Biogeochem. Cycles*, *12*, 311–320.
- Knippertz, P. (2003), Tropical-extratropical interactions causing precipitation in Northwest Africa: Statistical analysis and seasonal variations, *Mon. Weather Rev.*, *131*, 3069–3076.
- Knippertz, P., A. Fink, A. Reiner, and P. Speth (2003), Three late summer/early autumn cases of tropical-extratropical interactions causing precipitation in Northwest Africa, *Mon. Weather Rev.*, *131*, 161–135.
- Knippertz, P., C. Deutscher, K. Kandler, T. Müller, O. Schulz, and L. Schütz (2007), Dust mobilization due to density currents in the Atlas region: Observations from the SAMUM 2006 field campaign, *J. Geophys. Res.*, *112*, D21109, doi:10.1029/2007JD008774.
- Knippertz, P., et al. (2009a), Dust mobilization and transport in the Northern Sahara during SAMUM 2006—A meteorological overview, *Tellus, Ser. B*, *61*, 12–31.
- Knippertz, P., J. Trentmann, and A. Seifert (2009b), High-resolution simulations of convective cold pools over the northwestern Sahara, *J. Geophys. Res.*, *114*, D08110, doi:10.1029/2008JD011271.
- Koch, J., and N. Renno (2005), The role of convective plumes and vortices on the global aerosol budget, *Geophys. Res. Lett.*, *32*, L18806, doi:10.1029/2005GL023420.
- Lawrence, M. (2005), The relationship between relative humidity and the dewpoint temperature in moist air—A simple conversion and applications, *Bull. Am. Meteorol. Soc.*, *86*, 225–233.
- Lawson, T. (1971), Haboob structure at Khartoum, *Weather*, *26*, 105–112.
- Marshall, J. H., D. J. Parker, C. M. Grams, C. M. Taylor, and J. M. Haywood (2008), Uplift of Saharan dust south of the intertropical discontinuity, *J. Geophys. Res.*, *113*, D21102, doi:10.1029/2008JD009844.
- Membery, D. (1985), A gravity-wave haboob?, *Weather*, *40*, 214–221.
- Middleton, N., and A. Goudie (2001), Saharan dust: Sources and trajectories, *Trans. Inst. Br. Geogr.*, *26*(2), 165–181.
- Miller, S., A. Kuciauskas, M. Liu, Q. Ji, J. Reid, D. Breed, A. Walker, and A. Mandoos (2008), Haboob dust storms of the southern Arabian Peninsula, *J. Geophys. Res.*, *113*, D01202, doi:10.1029/2007JD008550.
- Min, Q.-L., R. Li, B. Lin, E. Joseph, S. Wang, Y. Hu, V. Morris, and F. Chang (2009), Evidence of mineral dust altering cloud microphysics and precipitation, *Atmos. Chem. Phys.*, *9*, 3223–3231.
- Offer, Z., and D. Goossens (2001), Ten years of aeolian dust dynamics in a desert region (Negev desert, Israel): Analysis of airborne dust concentration, dust accumulation and the high-magnitude dust events, *J. Arid Environ.*, *47*(2), 211–249.
- Schulz, O., and C. de Jong (2004), Snowmelt and sublimation: Field experiments and modelling in the High Atlas Mountains of Morocco, *Hydrol. Earth Syst. Sci.*, *8*(6), 1076–1089.

- Schulz, O., and M. Judex (Eds.) (2008), *IMPETUS Atlas Morocco: Research Results 2000–2007*, pp. 17–18, Univ. of Bonn, Bonn, Germany.
- Shinn, E., G. Smith, J. Prospero, P. Betzer, M. Hayes, V. Garrison, and R. Barber (2000), African dust and the demise of Caribbean coral reefs, *Geophys. Res. Lett.*, *27*(19), 3029–3032.
- Simpson, J. (1997), *Gravity Currents in the Environment and the Laboratory*, 244 pp., Halsted, Chichester, U. K.
- Smith, R., and M. Reeder (1988), On the movement and low-level structure of cold fronts, *Mon. Weather Rev.*, *116*, 1927–1944.
- Sutton, L. (1925), Haboobs, *Q. J. R. Meteorol. Soc.*, *51*, 25–30.
- Swap, R., M. Garstang, S. Greco, R. Talbot, and P. Kålberg (1992), Saharan dust in the Amazon Basin, *Tellus, Ser. B*, *44*, 133–149.
- Textor, C., et al. (2006), Analysis and quantification of the diversities of aerosol life cycles within AeroCom, *Atmos. Chem. Phys.*, *6*, 1777–1813.
- Weisman, M., and R. Rotunno (2004), ‘A theory for strong long-lived squall lines’ revisited, *J. Atmos. Sci.*, *61*(4), 361–382.
- Williams, E., N. Nathou, E. Hicks, C. Pontikis, B. Russell, M. Miller, and M. Bartholomew (2008), The electrification of dust-lofting gust fronts (‘haboobs’) in the Sahel, *Atmos. Res.*, *91*(2–4), 292–298, doi:10.1016/j.atmosres.2008.05.017.

C. Emmel, Department of Earth and Ocean Sciences, University of British Columbia, Vancouver, BC V6T 1Z4, Canada. (c Emmel@eos.ubc.ca)

P. Knippertz, Institute for Climate and Atmospheric Science, Faculty of Environment, School of Earth and Environment, University of Leeds, Leeds LS2 9JT, UK. (p.knippertz@leeds.ac.uk)

O. Schulz, Geographisches Institut, Universität Bonn, Meckenheimer Allee 166, D-53115 Bonn, Germany. (oschulz@uni-bonn.de)